Three-dimensional magnetohydrodynamics axisymmetric stagnation flow and heat transfer due to an axisymmetric shrinking/stretching sheet with viscous dissipation and heat source/sink*

Dinesh Rajotia† and R. N. Jat‡

Department of Mathematics, University of Rajasthan, Jaipur 302004, *India*

(Received 13 September 2013; revised manuscript received 20 November 2013; published online 22 May 2014)

The present work is concerned with the effects of viscous dissipation and heat source/sink on a three-dimensional magnetohydrodynamic boundary layer axisymmetric stagnation flow, and the heat transfer of an electrically conducting fluid over a sheet, which shrinks or stretches axisymmetrically in its own plane where the line of the symmetry of the stagnation flow and that of the shrinking (stretching) sheet are, in general, not aligned. The governing equations are transformed into ordinary differential equations by using suitable similarity transformations and then solved numerically by a shooting technique. This investigation explores the conditions of the non-existence, existence and uniqueness of the solutions of the similar equations numerically. It is noted that the range of the velocity ratio parameter, where the similarity solution exists, is increased with the increase of the value of the magnetic parameter. Furthermore, the study reveals that the non-alignment function affects the shrinking sheet more than the stretching sheet. In addition, the numerical results of the velocity profile, temperature profile, skin-friction coefficient, and rate of heat transfer at the sheet are discussed in detail with different parameters.

Keywords: axisymmetric shrinking/stretching sheet, stagnation-point flow, magnetic effect, heat transfer

PACS: 47.15.Cb, 47.65.–d, 44.20.+b **DOI:** 10.1088/1674-1056/23/7/074701

1. Introduction

The study of boundary layer flow over a stretching/shrinking sheet is a subject of great interest due to its various applications in the engineering process, such as plasma studies, petroleum industries, geothermal energy extractions, and in designing cooling systems, which includes liquid metals, magnetohydrodynamics (MHD) generators, accelerators, pumps and flow meters. Furthermore, the continuous surface heat and mass transfer problems are related to many practical applications in electrochemistry and polymer processing.

Stagnation flow, describing the fluid motion near the stagnation region, exists on all solid bodies moving in a fluid. The stagnation region encounters the highest pressure, the highest heat transfer and the highest rates of mass deposition. Hiemenz[1] was the first to study two-dimensional (2D) stagnation flow using a similarity transform to reduce the Navier–Stokes equations to non-linear ordinary differential equations. The axisymmetric case of the above problem was investigated by Homann.[2] On the other hand, the flow due to a stretching sheet, which is important in extrusion problems, also admits similarity solutions. Crane[3] was the first who found an exact similarity solution in closed analytic form for a steady 2D flow of an incompressible fluid over a stretching sheet where the velocity on the boundary is proportional to the distance. In addition, the studies of heat and mass transfer of the flow maintained at constant as well as variable wall temperature past a stretching sheet with suction were conducted by Gupta *et al.*[4] Wang[5] studied a steady three-dimensional (3D) flow of a viscous fluid over a plane surface which was stretched in its own plane in two lateral directions at different rates. Chiam[6] investigated a 2D steady stagnation-point flow of viscous fluid over a stretching surface. Consequently, the combination of both stagnation flow and stretching surface was considered by Mahapatra and Gupta[7,8] and extended to oblique stagnation flow by Lok *et al.*[9] The corresponding problem of axisymmetric stagnation flow towards a stretching surface in the presence of a uniform transverse magnetic field with heat generation was investigated by Attia.[10] Ding and Zhang[11] gave an analytic solution for a MHD stagnation point flow towards a stretching sheet. The similarity solution for an unsteady MHD stagnation-point flow of a 3D porous body with heat and mass transfer was investigated by Chamkha and Ahamed.[12] Further, dual solutions in boundary layer stagnation-point flow and mass transfer with the chemical reaction past a stretching/shrinking sheet were given by Bhattacharyya.[13] Consequently, Bhattacharyya *et al.*[14] reported on the slip effects on an unsteady boundary layer stagnation-point flow and heat transfer towards a stretching sheet. The effects of partial slip and variable fluid viscosity on a stagnation flow past a stretching sheet in the presence of a heat source/sink were reported by Mukhopadhyay *et al.*[15]

*Project supported by the C.S.I.R., India in the form of Junior Research Fellowship (JRF) (Grant No. 09/149(0593) /2011-EMR-I).

†Corresponding author. E-mail: rajotia.dinesh@gmail.com

‡Corresponding author. E-mail: khurkhuria_rnjat@yahoo.com

© 2014 Chinese Physical Society and IOP Publishing Ltd

Recently, the boundary layer flow due to a shrinking sheet has attracted more considerable interest. Miklavcic and Wang[16] investigated a 2D and axisymmetric viscous flow induced by a shrinking sheet in the presence of uniform suction, and they found that the existence of the similarity solutions is possible in a certain range of the suction parameter. The above shrinking sheet problem was extended to power-law surface velocity by Fang.[17] Fang and Zhang[18] gave an exact solution of MHD boundary layer equations in the closed analytical form for the flow of an electrically conducting fluid. Fang *et al.*[19] studied the viscous flow over an unsteady shrinking sheet with mass transfer. Ishak *et al.*[20] investigated a magnetohydrodynamic flow towards a permeable surface with a prescribed wall heat flux. Further, the slip MHD viscous flow over a permeable shrinking sheet was investigated by Fang *et al.*[21] Alsaedi *et al.*[22] gave an analytic solution for the MHD boundary layer flow of Casson fluid over a stretching/shrinking sheet with wall mass transfer. A steady 2D and axisymmetric stagnation-point flow with heat transfer on a shrinking sheet was investigated by Wang[23] and he found that with an added stagnation-point flow to contain the vorticity, a similarity solution is possible even in the absence of suction at the surface. Rahimpour *et al.*[24] gave the analytical solution of axisymmetric stagnation flow towards a shrinking sheet. Recently, Mahapatra *et al.*[25] studied a steady 2D MHD stagnation-point flow of an electrically conducting incompressible viscous fluid over a shrinking sheet, the flow being permeated by a uniform transverse magnetic field. Bhattacharyya and Layek[26] investigated the effects of suction/blowing on steady boundary layer stagnation-point flow and heat transfer towards a shrinking sheet with thermal radiation. Consequently, dual solutions in an unsteady stagnation-point flow over a shrinking sheet were given by Bhattacharyya.[27] Bhattacharyya *et al.*[28] also investigated the slip effects on boundary layer stagnation-point flow and heat transfer towards a shrinking sheet. The heat transfer stagnation flow problem with non-uniform heat flux was recently discussed again by Bhattacharyya.[29]

In the present investigation, our objective is to study the three-dimensional (3D) MHD boundary layer axisymmetric stagnation flow and the heat transfer of an electrically conducting fluid past an axisymmetric shrinking/stretching sheet with viscous dissipation and heat source/sink where the line of the symmetry of stagnation flow and that of the shrinking (stretching) sheet are not aligned. Actually, this investigation is an extension of the problem studied by Wang,[23] of axisymmetric flow over an axisymmetric shrinking sheet taking the magnetic effect into account in the presence of the viscous dissipation and heat source/sink.

2. Formulation of the problem

Consider a 3D and axisymmetric stagnation flow of an electrically conducting incompressible viscous fluid towards a sheet which shrinks or stretches axisymmetrically in its own plane (Fig. 1). The velocity components u, v and w are taken along the x, y, and z directions, respectively, where the x and y axes are along the length and breadth of the sheet and the z axis is perpendicular to the sheet. On the surface of the sheet, the velocity components are

$$u = U_{\rm w}(x) = b(x+c), \quad v = V_{\rm w}(y) = \alpha a y, \quad w = 0, \tag{1}$$

where $b < 0$ is the shrinking rate, $b > 0$ is the stretching rate, $-c$ is the location of the shrinking (stretching) origin, a is the strength of stagnation flow, and $\alpha = b/a$ is the velocity ratio parameter or the ratio of the stretching (shrinking) rate to the strength of stagnation flow. Here, the line of the symmetry of stagnation flow and that of the shrinking (stretching) sheet are, in general, not aligned ($c \neq 0$). A constant magnetic field with strength B_0 is applied in the z direction. The magnetic Reynolds number is taken to be small, so that the induced magnetic field is neglected.

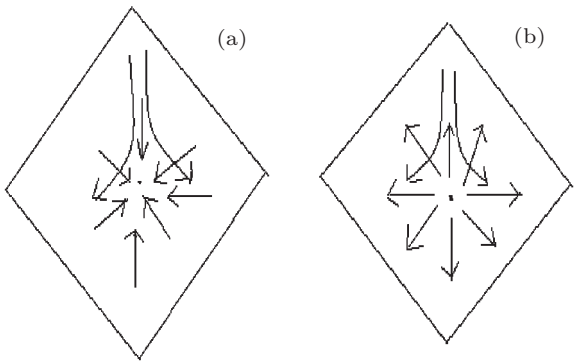


Fig. 1. Systematic diagram of physical model, showing (a) axisymmetric stagnation flow on axisymmetric shrinking sheet, and (b) axisymmetric stagnation flow on axisymmetic stretching sheet.

Under the usual boundary layer approximations, the basic governing boundary layer equations of continuity and momentum (Wang[23]) are

$$\frac{\partial u}{\partial x} + \frac{\partial v}{\partial y} + \frac{\partial w}{\partial z} = 0, \tag{2}$$

$$u\frac{\partial u}{\partial x} + v\frac{\partial u}{\partial y} + w\frac{\partial u}{\partial z} = -\frac{1}{\rho}\frac{\partial p}{\partial x} + \nu\left(\frac{\partial^2 u}{\partial z^2}\right) - \frac{\sigma B_0^2}{\rho}u, \tag{3}$$

$$u\frac{\partial v}{\partial x} + v\frac{\partial v}{\partial y} + w\frac{\partial v}{\partial z} = -\frac{1}{\rho}\frac{\partial p}{\partial y} + \nu\left(\frac{\partial^2 v}{\partial z^2}\right) - \frac{\sigma B_0^2}{\rho}v, \tag{4}$$

where $\nu = \mu/\rho$ is the kinematic viscosity, μ is the dynamic viscosity, ρ is the density of the fluid, p is the pressure, σ is the electrical conductivity, and B_0 is the magnetic induction.

In the inviscid free stream $u = U_\infty(x) = ax$, $v = V_\infty(y) = ay$ and one can write

$$U_\infty\frac{\partial U_\infty}{\partial x} + \frac{\sigma B_0^2}{\rho}U_\infty = -\frac{1}{\rho}\frac{\partial p}{\partial x}, \tag{5}$$

$$V_\infty \frac{\partial V_\infty}{\partial y} + \frac{\sigma B_0^2}{\rho} V_\infty = -\frac{1}{\rho}\frac{\partial p}{\partial y}. \tag{6}$$

Then by eliminating $\partial p/\partial x$ and $\partial p/\partial y$, the momentum equations (3) and (4) are reduced, respectively, to

$$\begin{aligned} &u\frac{\partial u}{\partial x} + v\frac{\partial u}{\partial y} + w\frac{\partial u}{\partial z} \\ &= U_\infty \frac{\partial U_\infty}{\partial x} + \nu\left(\frac{\partial^2 u}{\partial z^2}\right) - \frac{\sigma B_0^2}{\rho}(u - U_\infty), \end{aligned} \tag{7}$$

$$\begin{aligned} &u\frac{\partial v}{\partial x} + v\frac{\partial v}{\partial y} + w\frac{\partial v}{\partial z} \\ &= V_\infty \frac{\partial V_\infty}{\partial y} + \nu\left(\frac{\partial^2 v}{\partial z^2}\right) - \frac{\sigma B_0^2}{\rho}(v - V_\infty). \end{aligned} \tag{8}$$

The energy equation for axisymmetric flow with viscous and Ohmic dissipations and heat source/sink is given as

$$\begin{aligned} &u\frac{\partial T}{\partial x} + v\frac{\partial T}{\partial y} + w\frac{\partial T}{\partial z} \\ &= \frac{\kappa}{\rho c_\mathrm{p}}\left(\frac{\partial^2 T}{\partial x^2} + \frac{\partial^2 T}{\partial y^2} + \frac{\partial^2 T}{\partial z^2}\right) \\ &\quad + \frac{Q_0(T - T_\infty)}{\rho c_\mathrm{p}} + \frac{\sigma B_0^2}{\rho c_\mathrm{p}}\{(u - U_\infty) + (v - V_\infty)\} \\ &\quad + \frac{\mu}{\rho c_\mathrm{p}}\left\{2\left[\left(\frac{\partial u}{\partial x}\right)^2 + \left(\frac{\partial v}{\partial y}\right)^2 + \left(\frac{\partial w}{\partial z}\right)^2\right]\right. \\ &\quad \left. + \left(\frac{\partial u}{\partial y} + \frac{\partial v}{\partial x}\right)^2 + \left(\frac{\partial u}{\partial z} + \frac{\partial w}{\partial x}\right)^2 + \left(\frac{\partial v}{\partial z} + \frac{\partial w}{\partial y}\right)^2\right\}, \end{aligned} \tag{9}$$

where T is the temperature of the fluid, T_∞ is the free stream temperature, κ is the thermal conductivity, c_p is the specific heat at constant pressure, and Q is the volumetric rate of heat source or sink.

The boundary conditions applicable to the present flow are

$$\begin{aligned} &z = 0: \quad u = b(x + c), \quad v = \alpha a y = by, \quad w = 0, \quad T = T_\mathrm{w}, \\ &z \to \infty: \quad u \to U_\infty(x) = ax, \quad v \to V_\infty(y) = ay, \quad T \to T_\infty, \end{aligned} \tag{10}$$

where the temperature at the sheet is T_w.

3. Analysis

Introducing the following similarity transformations:

$$\begin{aligned} &u = axf'(\eta) + bch(\eta), \quad v = ayf'(\eta), \quad w = -2\sqrt{a\nu}f(\eta), \\ &\theta(\eta) = \frac{T - T_\infty}{T_\mathrm{w} - T_\infty}, \quad \text{and} \quad \eta = \sqrt{\frac{a}{\nu}}z. \end{aligned} \tag{11}$$

Equation (2) is identically satisfied by similarity transformations while Eqs. (7)–(9) become

$$f''' + 2ff'' - f'^2 + M(1 - f') + 1 = 0, \tag{12}$$

$$h'' + 2fh' - hf' - Mh = 0, \tag{13}$$

$$\begin{aligned} &\theta'' + Pr\left[2f\theta' + Q\theta + 12Ecf'^2 + (Ec_x + Ec_y)\right. \\ &\quad \times \left\{f''^2 + (f' - 1)^2\right\} + \alpha^2 Ec_x \frac{Re'}{Re}\left(h'^2 + Mh^2\right) \\ &\quad \left. + 2\alpha Ec_x\sqrt{\frac{Re'}{Re}}\left\{h'f'' + Mh(f' - 1)\right\}\right] = 0. \end{aligned} \tag{14}$$

Corresponding boundary conditions are

$$\begin{aligned} &\eta = 0: \quad f = 0, \quad f' = \alpha = b/a, \quad h = 1, \quad \text{and} \quad \theta = 1, \\ &\eta \to \infty: \quad f' \to 1, \quad h \to 0, \quad \text{and} \quad \theta \to 0, \end{aligned} \tag{15}$$

where a prime denotes differentiation with respect to similarity variable η, $M = \sigma B_0^2/\rho a$ is the magnetic parameter, $Pr = \mu c_\mathrm{p}/\kappa$ is the Prandtl number, $Q = Q_0/a\rho c_\mathrm{p}$ is the heat Source ($Q > 0$) or sink ($Q < 0$) parameter

$$Ec = \frac{\mu a}{\rho c_\mathrm{p}(T_\mathrm{w} - T_\infty)}$$

is the Eckert number, $Re' = c^2 a/\nu$ and $Re = ax^2/\nu$ are the Reynolds numbers,

$$Ec_x = \frac{a^2x^2}{c_\mathrm{p}(T_\mathrm{w} - T_\infty)} \quad \text{and} \quad Ec_y = \frac{a^2y^2}{c_\mathrm{p}(T_\mathrm{w} - T_\infty)}$$

are the local Eckert numbers based on the variables x and y, respectively.

4. Numerical method for solution

The set of nonlinear ordinary differential equations (12)–(14) with boundary conditions (15) form a boundary value problem (BVP) and can be solved numerically by converting them into an initial value problem (IVP) using the shooting method. We set the following first-order system:

$$f' = z, \quad z' = p,$$

$$p' = -2fp + z^2 - M(1 - z) - 1, \tag{16}$$

$$h' = q, \quad q' = -2fq + hz + Mh, \tag{17}$$

$$\begin{aligned} \theta' &= r, \\ r' &= -Pr\left\{2fr + Q\theta + 12Ecz^2 + (Ec_x + Ec_y)\right. \\ &\quad \times \left[p^2 + (z - 1)^2\right] + \alpha^2 Ec_x \frac{Re'}{Re}\left(q^2 + Mh^2\right) \\ &\quad \left. + 2\alpha Ec_x\sqrt{\frac{Re'}{Re}}\left[qp + Mh(z - 1)\right]\right\}, \end{aligned} \tag{18}$$

with boundary conditions

$$f(0) = 0, \quad z(0) = \alpha, \quad h(0) = 1, \quad \theta(0) = 1. \tag{19}$$

In order to integrate Eqs. (16)–(18) with (19) as an initial value problem (IVP), one requires a value for $p(0)$ i.e.,$f''(0)$ and $q(0)$ i.e., $h'(0)$ and $r(0)$ i.e., $\theta'(0)$ but no such values are given in the problem. Now, choosing the suitable initial guesses for $f''(0)$, $h'(0)$, and $\theta'(0)$ and using the fourth order Runge–Kutta method to solve the IVP, a solution is obtained.

Comparing the calculated values of $f'(\eta)$, $h(\eta)$, and $\theta(\eta)$ at η_∞ (a suitable finite value of $\eta \to \infty$) with the given boundary conditions $f'(\eta_\infty) = 1$, $h(\eta_\infty) = 0$, and $\theta(\eta_\infty) = 0$, and adjusting the estimated values of $f''(0)$, $h'(0)$, and $\theta'(0)$ using the Secant method to obtain a better approximation for the solution. The step-size is taken as $\Delta\eta = 0.001$. The above procedure is repeated until we obtain the converged results within a tolerance limit of 10^{-7}. All the computations are done by generating a program in Matlab software.

5. Results and discussion

In order to analyze the results of velocity profile $f'(\eta)$, temperature profile $\theta(\eta)$, skin friction coefficients $f''(0)$ and $h'(0)$, and the rate of heat transfer at the surface $-\theta'(0)$, all the numerical computations are carried out for various values of the velocity ratio parameter α, magnetic parameter M, Prandtl number Pr, heat source/sink parameter Q, Eckert number Ec and local Eckert numbers Ec_x and Ec_y.

First of all, we compare the local skin friction coefficients $f''(0)$, $h'(0)$ and the rate of heat transfer at the sheet $-\theta'(0)$ in the absence of a magnetic field, i.e., $(M = 0)$ for different values of α with the available results of Wang[23] and Rahimpour *et al.*[24] Wang[23] numerically solved the axisymmetric stagnation flow problem over an axisymmetric shrinking sheet in the absence of a magnetic field and Rahimpour *et al.*[24] solved the same problem analytically. The results of $f''(0)$ and $h'(0)$ for the stretching $(\alpha > 0)$ and shrinking $(\alpha < 0)$ cases are given in Tables 1 and 2, respectively. From both cases, the solutions seem to be unique for $\alpha \geq -1$ and no solutions are found for $\alpha < -1$ in the absence of the magnetic field. Notice that here $\alpha = 0$ presents the axisymmetric stagnation flow towards a solid plate and $\alpha = 1$ corresponds to inviscid flow with no boundary layer. The results of $-\theta'(0)$ for the stretching $(\alpha > 0)$ and shrinking $(\alpha < 0)$ cases are given in Table 3. All these results show that they are in favorable agreement with the results of (Wang[23] and Rahimpour *et al.*[24]) and thus give confidence that the obtained numerical results are accurate, so we can proceed to further analysis.

Table 1. Initial values for axisymmetric stretching sheet case when $M = 0$.

α	$f''(0)$			$h'(0)$		
	Wang[23]	Rahimpour[24]	Present	Wang[23]	Rahimpour[24]	Present
0	1.31193	1.311938	1.311937	–0.93873	–0.938732	–0.936972
0.1	1.22911	1.229113	1.229112	–1.00400	–1.004026	–1.002212
0.5	0.78032	0.780323	0.780323	–1.2355	–1.235451	–1.233402
1	0.0	0.0	0.0	–1.4793	–1.479337	–1.476965
2	–2.13107	–2.131069	–2.131066	–1.8800	–1.879949	–1.876887
5	–11.8022	–11.80221	–11.80221	–2.7617	–2.761702	–2.756425

Table 2. Initial values for axisymmetric shrinking sheet case when $M = 0$.

α	$f''(0)$			$h'(0)$		
	Wang[23]	Rahimpour[24]	Present	Wang[23]	Rahimpour[24]	Present
–0.25	1.45664	1.45659	1.45663	–0.75639	–0.756390	–0.754748
–0.5	1.49001	1.49000	1.49001	–0.53237	–0.532371	–0.530805
–0.75	1.35284	1.35285	1.35284	–0.22097	–0.220789	–0.219208
–0.95	0.94690	0.94681	0.94710	0.26845	0.268450	0.270035

Table 3. Values of rate of heat transfer at sheet with $M = 0$.

α	$-\theta'(0)$			
	$Pr = 0.7$		$Pr = 7$	
	Rahimpour[24]	Present	Rahimpour[24]	Present
1.0	0.94406	0.942291	2.98541	2.967663
0.5	0.81676	0.815455	2.34510	2.334163
0.0	0.66540	0.664513	1.54570	1.541020
–0.25	0.57485	0.574218	1.05649	1.054251
–0.50	0.46709	0.466750	0.51204	0.511507
–0.75	0.32600	0.326142	0.07191	0.071896
–0.95	0.13688	0.139908	0.00003	0.000003

Figure 2 shows the trajectories of the values of $f''(0)$ and $h'(0)$ against α for different values of the magnetic parameter M. From the figure, we observe that in the absence of the magnetic parameter ($M = 0$), the solutions of Eqs. (12) and (13) for $f(\eta)$ and $h(\eta)$ satisfying the boundary condition (15), are unique for $\alpha \geq -1$ and no similarity solution exists for $\alpha < -1$. These results agree well with those of Wang.[23] When $\alpha = 1$, we find that $f''(0)$ becomes zero for all values of M while $f''(0) \geq 0$ in a range of $-1 \leq \alpha \leq 1$ and with a fixed value of α, $f''(0)$ increases with the augmentation of M. While the trajectory for $h'(0)$ crosses the α axis in the case of flow over a shrinking sheet but it does not cross the α-axis for flow over a stretching sheet. The magnitude of $h'(0)$ decreases with the increase of α with a fixed value of M, while for a given value of α, it also decreases with the increase of M. Consequently, a major result emerging from the analysis is that as M increases, the range of α where similarity solutions exist continuously increases. This result reveals that the existence and the uniqueness of the similarity solution depend not only on the parameter α but also on the magnetic parameter M.

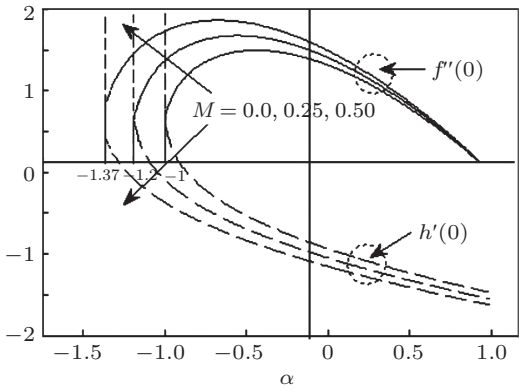


Fig. 2. Variations of $f''(0)$ and $h'(0)$ with α for various values of M.

In addition, the exact values of velocity ratio parameter α upto which the similarity solution exists for a specific increased value of M are listed in Table 4. We observe that for $M = 0.25$, the similarity solutions seem to be unique for $\alpha \geq -1.20$ and no solutions are found for $\alpha < -1.20$. While in the case of $M = 0.5$, the similarity solutions exist uniquely for $\alpha \geq -1.37$ and no solutions are found for $\alpha < -1.37$.

The universal curves of function $f(\eta)$ against η for different values of α are shown in Fig. 3 in the presence of a magnetic field i.e., $M = 0.5$. It is found that all curves of $f(\eta)$ start from the origin and approach identical slopes for a large value of η. When $\alpha = 1$, the flow is inviscid and no boundary layers are needed. The case $\alpha = 0$ gives the axisymmetric stagnation flow towards a solid plate. For all shrinking cases ($\alpha < 0$), the function $f(\eta)$ is initially negative, showing regions of reverse cellular flow. Figure 4 shows the variations of the non-alignment function $h(\eta)$ with η for different values of α with $M = 0.5$. It is seen that with the increasing of the strength of shrinking ($\alpha < 0$) of the sheet, the non-alignment function $h(\eta)$ increases while it decreases with the increasing of the strength of the stretching ($\alpha > 0$) rate. In addition, we can easily see that the effect of the non-alignment function is small for the stretching sheet but large for the shrinking sheet.

Table 4. Values of $f''(0)$, $h'(0)$, and $-\theta'(0)$ in the presence of M with $Pr = 0.7$, $Ec = 0 = Q$.

M	α	$f''(0)$	$h'(0)$	$-\theta'(0)$
0.25	1	0	–1.55467	0.942291
	0.5	0.818293	–1.32417	0.817906
	0	1.402364	–1.05004	0.671920
	–0.5	1.670827	-0.69483	0.487568
	–1	1.363586	–0.09324	0.201653
	–1.15	0.910221	0.352313	0.047733
	–1.195	0.587697	0.656125	0.005212
	–1.20	0	inf	0
0.50	1	0	–1.629235	0.942291
	0.5	0.854711	-1.410085	0.821795
	0	1.487651	–1.154275	0.678545
	–0.5	1.833036	-0.835762	0.504562
	–1	1.727356	-0.793730	0.262195
	–1.2	1.431895	–0.064226	0.121794
	–1.3	1.147821	0.175314	0.041658
	–1.35	0.938400	0.339154	0.011999
	–1.365	0.864541	0.394649	0.006583
	–1.37	0	inf	0

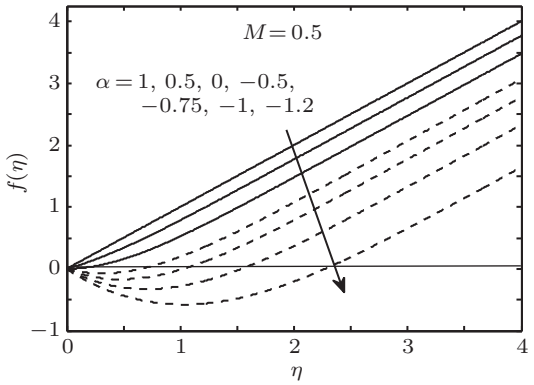


Fig. 3. Variations of $f(\eta)$ against η for various values of α.

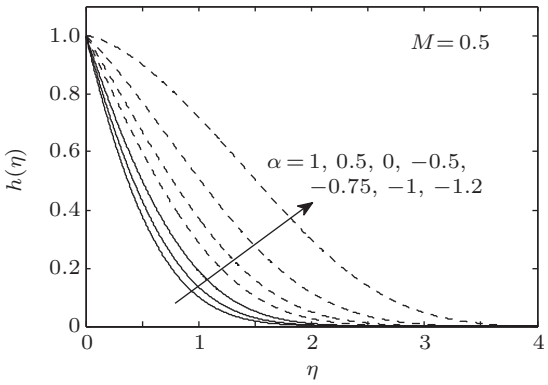


Fig. 4. Variations of $h(\eta)$ against η for various values of α.

The variations of the function $f(\eta)$ with η for different values of M for both cases of shrinking and stretching rates are shown in Fig. 5. It is found that for shrinking at the surface ($\alpha < 0$), the function $f(\eta)$ is negative near the shrinking sheet showing regions of reverse cellular flow and also, as the M increases, the region of reverse cellular flow decreases. For stretching at the surface ($\alpha > 0$), the function $f(\eta)$ is not much changed near the surface of the sheet with M while after a certain distance normal to the sheet, it increases slowly with M. Figure 6 shows the variation of the velocity profile $f'(\eta)$ against η for different values of M with both cases of the sheet. It is observed that as M increases, the velocity profile increases more for the shrinking case ($\alpha = -0.5$) than for the stretching case ($\alpha = 0.25$). Figure 7 exhibits the effects of M on the non-alignment function $h(\eta)$ in the presence of the shrinking ($\alpha < 0$) and stretching ($\alpha > 0$) of the sheet. With the increasing of the value of M, the non-alignment function $h(\eta)$ decreases in both cases of the shrinking ($\alpha < 0$) and stretching ($\alpha > 0$) of the sheet. In addition, it is evident to conclude that the effect of the non-alignment function becomes less with the increasing of the value of M for both cases of the sheet.

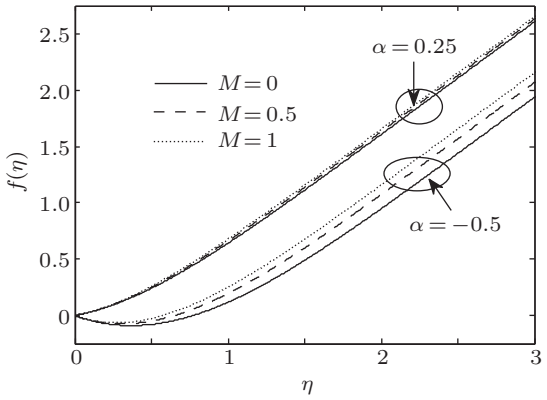


Fig. 5. Variations of $f(\eta)$ against η for various values of M.

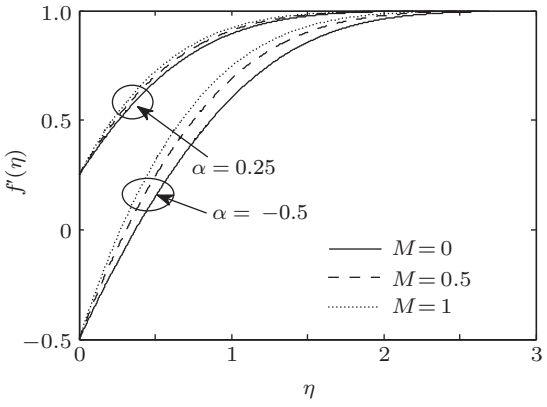


Fig. 6. Velocity profiles against η for various values of M.

Figure 8 presents the effects of M on the temperature profile for both cases of the sheet. For shrinking of the sheet ($\alpha = -0.5$), the temperature profile decreases with the increasing of the value of M. On the other hand, for the stretching of the sheet ($\alpha = 0.5$), the temperature profile does not change much with M. Figure 9 shows the effects of the parameter α on the temperature profile in the presence of the magnetic field ($M = 0.5$). It is found that with the increase of the strength of shrinking ($\alpha < 0$), the temperature profile also increases very smoothly while in the case of increasing the strength of stretching ($\alpha > 0$), the temperature profile gives the reverse phenomena in comparison to the shrinking of the sheet i.e., it decreases.

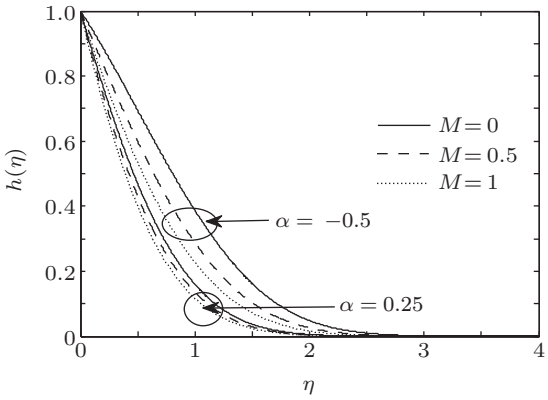


Fig. 7. Variations of $h(\eta)$ against η for various values of M.

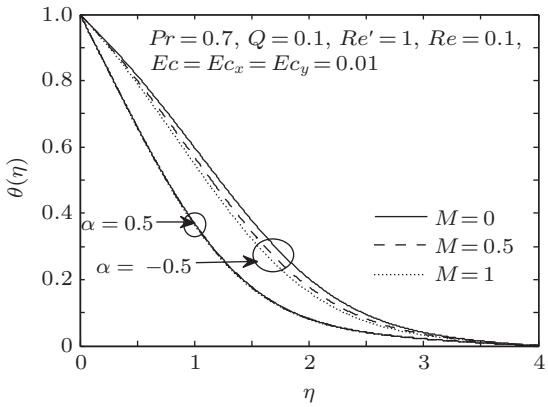


Fig. 8. Temperature profiles against η for various values of M.

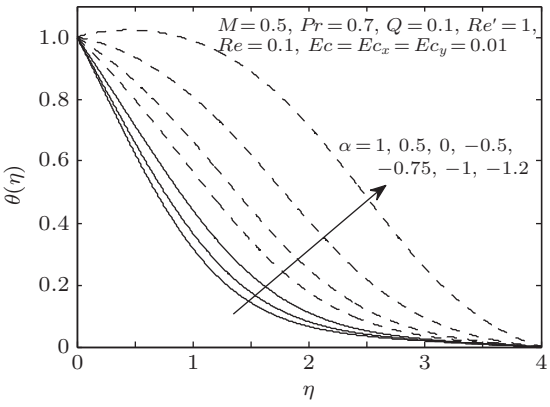


Fig. 9. Temperature profiles against η for various values of α.

The effects of Prandtl number Pr on the temperature profile for both cases are described in Fig. 10. It is seen that initially the temperature of the fluid increases and after a certain distance normal to the shrinking sheet, it decreases with the increasing of the value of Pr. On the other hand, in the case of the stretching sheet, the temperature of the fluid as well as the thermal boundary layer thickness decreases with the increase of Prandtl number Pr. This happens because when Pr increases, the thermal conductivity decreases, thus it leads to the decrease of the energy transfer ability. Figure 11 presents the effects of heat source/sink parameter Q on the temperature profile in the presence of the shrinking $(\alpha < 0)$ and stretching $(\alpha > 0)$ of the sheet. From both cases of shrinking and stretching of the sheet, it is found that the temperature of the fluid decreases with the increasing of strength of heat sink $Q < 0$ while due to the increase of the strength of the heat source $Q > 0$, the temperature profile increases. Therefore, the thickness value of the thermal boundary layer reduces with the increasing of the heat sink but it increases with the increasing values of the heat source parameter.

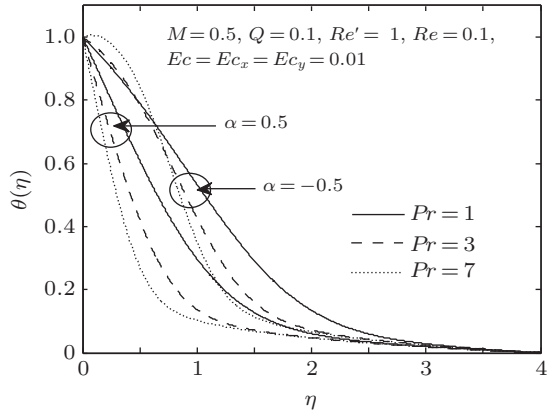


Fig. 10. Temperature profiles against η for various values of Pr.

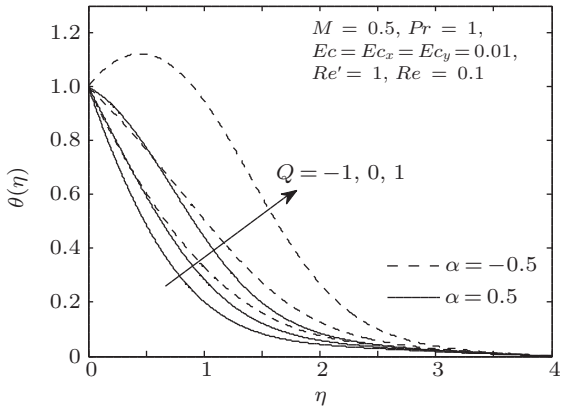


Fig. 11. Temperature profiles against η for various values of Q.

Effects of Eckert number Ec on the temperature profile on both cases of the sheet are shown in Fig. 12. It is noticed that by increasing the value of Ec, the temperature and the thermal boundary layer thickness value increase in both cases. Effects of local Eckert numbers Ec_x and Ec_y on the temperature profile are displayed in Figs. 13 and 14, respectively. From both figures, it is noticed that in the case of the shrinking sheet, the temperature of the fluid increases faster near the surface than far from the sheet with an increase of the values of Ec_x and Ec_y. This happens because the viscous dissipation creates frictional heating, which is stored in fluid as heat energy and thus it leads to the increase of the energy transfer ability, also in the case of stretching, the temperature of the fluid increases slowly with the increased values of Ec_x and Ec_y.

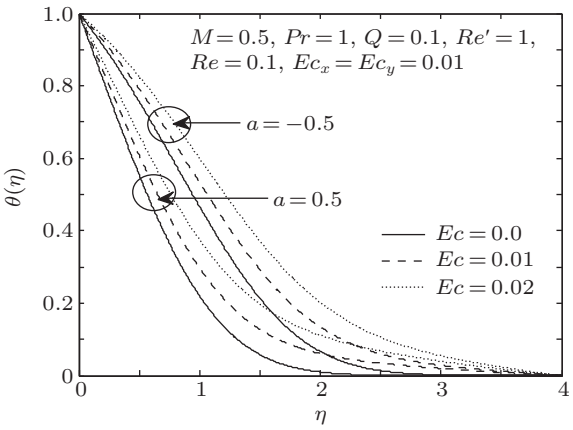


Fig. 12. Temperature profiles against η for various values of Ec.

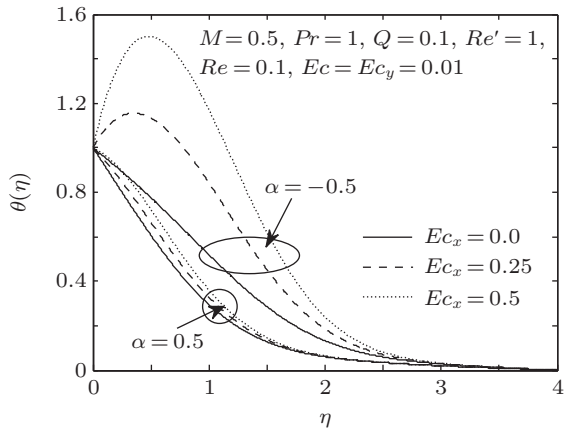


Fig. 13. Temperature profiles against η for various values of Ec_x.

Figure 15 shows variations of the temperature gradient at the sheet i.e. $-\theta'(0)$ (which is proportional to the rate of heat transfer from the sheet) with parameter α for different values of Pr and M with $Q = Ec = 0$. In the case of the stretching sheet, it is noticed that for both values of the magnetic parameter i.e., $M = 0, 0.5$, the rate of heat transfer $-\theta'(0)$ increases with the increase of the value of Pr. While in the case of the shrinking sheet, the parameter α causes a much larger change

in the heat transfer for water ($Pr = 7$) than for air ($Pr = 0.7$). In addition, the rate of heat transfer $-\theta'(0)$ increases with the increase on the values of α and M.

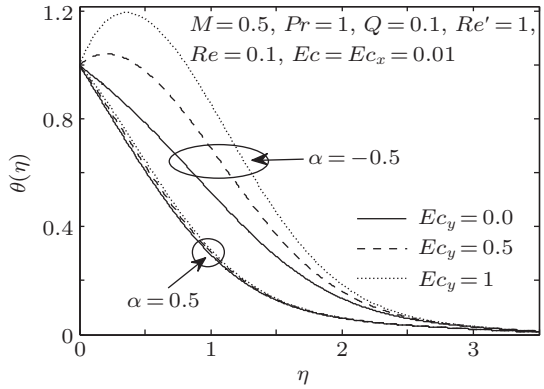


Fig. 14. Temperature profiles against η for various values of Ec_y.

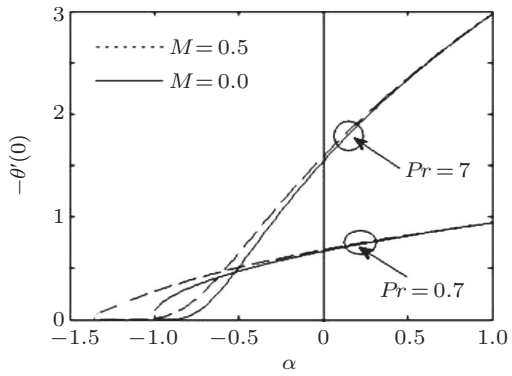


Fig. 15. Variations of $-\theta'(0)$ against α for different values of Pr and M.

The variations of the temperature gradient at the sheet i.e., $-\theta'(0)$ with α for different values of Q and Ec are depicted in Figs. 16 and 17. Both the figures indicate that the rate of heat transfer $-\theta'(0)$ decreases with the increasing of the values of Q and Ec, while it increases with the increasing of the value of α.

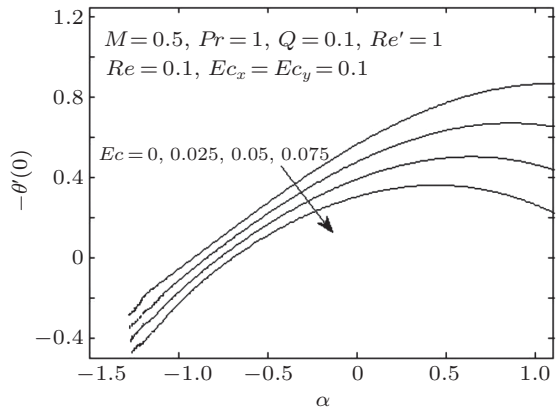


Fig. 16. Variations of $-\theta'(0)$ with α for various values of Ec.

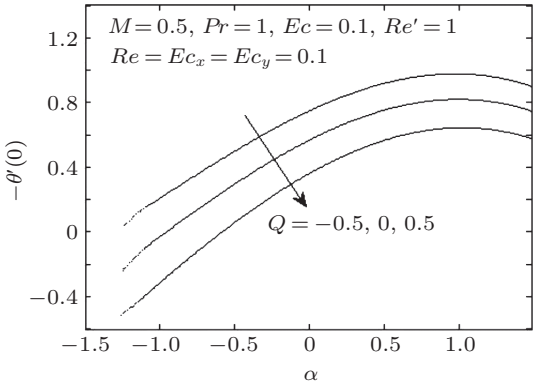


Fig. 17. Variations of $-\theta'(0)$ with α for various values of Q.

6. Conclusions

In the present work, we attempt to express the effects of viscous dissipations and heat source/sink on 3D MHD boundary layer axisymmetric stagnation flow and the heat transfer of an electrically conducting incompressible viscous fluid past an axisymmetric shrinking sheet by comparison with the axisymmetric stretching sheet. The symmetry line of the stagnation flow and that of the sheet are non-aligned and the effect of non-alignment is also studied. The set of nonlinear ordinary differential equations is solved numerically using the Runge–Kutta fourth-order algorithm with the shooting technique. Numerically, it is observed that with the increasing of the value of magnetic parameter, the certain domain of the velocity ratio parameter where the similarity solution exists also increases. In the case of the shrinking sheet, the region of reverse cellular flow is observed near the sheet and as the magnetic parameter increases, the region of reverse cellular flow decreases. On the other hand, the flow for the stretching sheet is not much affected with the magnetic parameter. The effect of a non-alignment stagnation flow is found to be small for the stretching sheet, but large for the shrinking sheet. The thermal boundary layer thickness increases with the increase of the values of Eckert number and heat source/sink while it decreases with the increase of velocity ratio parameter, magnetic parameter and Prandtl number in both cases of shrinking and stretching of the sheet. Therefore, the rate of heat transfer at the sheet decreases with the increase of the values of the heat source/sink parameter and Eckert number, while it increases with the increase of the velocity ratio parameter, magnetic parameter, and Prandtl number. Overall, the study remarks that in comparison to the stretching sheet, the shrinking sheet has many unique characteristics.

References

[1] Hiemenz K 1911 *Ding. Polytech. J.* **326** 321
[2] Homann F 1936 *Zeit. Angew. Math. Phys.* **16** 153

[3] Crane L J 1970 *Zeit. Angew. Math. Phys.* **21** 645
[4] Gupta P S and Gupta A S 1977 *Can. J. Chem. Eng.* **55** 744
[5] Wang C Y 1984 *Phys. Fluids* **27** 1915
[6] Chiam T C 1994 *J. Phys. Soc. Jpn.* **63** 2443
[7] Mahapatra T R and Gupta A S 2002 *Heat Mass Transfer* **38** 517
[8] Mahapatra T R and Gupta A S 2003 *Can. J. Chem. Eng.* **81** 258
[9] Lok Y Y, Amin N and Pop I 2006 *Int. J. Nonlinear Mech.* **41** 622.
[10] Attia H A 2007 *Tamkang J. Sci. Eng.* **10** 11
[11] Ding Q and Zhang H Q 2009 *Chin. Phys. Lett.* **26** 104701
[12] Chamkha A J and Ahmed S E 2011 *J. Appl. Fluid Mech.* **4** 87
[13] Bhattacharyya K 2011 *Int. Commun. Heat Mass Transfer* **38** 917
[14] Bhattacharyya K, Mukhopadhyay S and Layek G C 2011 *Chin. Phys. Lett.* **28** 094702
[15] Bhattacharyya K, Mukhopadhyay S and Layek G C 2012 *Acta Technica* **57** 183
[16] Miklavcic M and Wang C Y 2006 *Quarterly Applied Mathematics* **64** 283
[17] Fang T 2008 *Int. J. Heat Mass Transfer* **51** 5838
[18] Fang T and Zhang J 2009 *Commun. Nonlinear Sci. Numer. Simulat.* **14** 2853
[19] Fang T, Zhang J and Yao S S 2009 *Chin. Phys. Lett.* **26** 014703
[20] Ishak A, Nazar R and Pop I 2009 *Chin. Phys. Lett.* **26** 014702
[21] Fang T, Zhang J and Yao S S 2010 *Chin. Phys. Lett.* **27** 124702
[22] Alsaedi A, Hayat T and Bhattacharyya K 2013 *Chin. Phys. B* **22** 024702
[23] Wang C Y 2008 *Int. J. Nonlinear Mech.* **43** 377
[24] Rahimpour M, Mohebpour S R, Kimiaeifar A and Bagheri G H 2008 *Int. J. Mech.* **1** 1
[25] Mahapatra T R, Nandy S K and Gupta A S 2011 *J. Appl. Mech.* **78** 021015
[26] Bhattacharyya K and Layek G C 2011 *Int. J. Heat Mass Transfer* **54** 302
[27] Bhattacharyya K 2011 *Chin. Phys. Lett.* **28** 084702
[28] Bhattacharyya K, Mukhopadhyay S and Layek G C 2011 *Int. J. Heat Mass Transfer* **54** 308
[29] Bhattacharyya K 2013 *Chin. Phys. B* **22** 074705